

Code: _____



Faculty of Engineering and Sustainable Development

Measuring flow in digital video containing smoke and gas

Yunyi Huang
June 2011

Bachelor Thesis, 15 credits, C
Computer Science

Computer Science Program
Examiner: Stefan Seipel
Supervisor: Julia Åhlén

Measuring flow in digital video containing smoke and gas

by

Yunyi Huang

Faculty of Engineering and Sustainable Development
University of Gävle

S-801 76 Gävle, Sweden

Email:

ofk09yhg@student.hig.se

Abstract

Optical flow is widely used in image and video processing. This paper describes the definition of optical flow and some basic methods of estimating optical flow. There are three main optical flow methods described in this paper: Horn–Schunck method, Lucas–Kanade method and Anandan method. It will select the most appropriate method to measure the flow in videos containing smoke and gas by comparing those three methods with different criteria. The results are as below 1) Horn–Schunck method is good at measuring flow in infrared video and in horizontal direction, when 2) Anandan method is adept in estimating upward optical flow but not suitable for infrared video. 3) Lucas-Kanade method can be used not only in smoke videos, but also in methane gas videos, and it can detect flow in both horizontal and vertical direction.

Keywords: optical flow, video processing, smoke or gas detection

Contents

1	Introduction	1
1.1	Aim	2
1.2	Background	2
1.2.1	<i>Optical flow constraint equation.....</i>	<i>2</i>
1.2.2	<i>Aperture problem.....</i>	<i>3</i>
1.2.3	<i>Horn–Schunck method.....</i>	<i>3</i>
1.2.4	<i>Lucas–Kanade method.....</i>	<i>4</i>
1.2.5	<i>Pyramid Lucas-Kanade method.....</i>	<i>4</i>
1.2.6	<i>Anandan method</i>	<i>5</i>
1.2.7	<i>Angular error.....</i>	<i>5</i>
2	Comparative method.....	6
2.1	Selection of videos	6
2.2	Criteria.....	6
2.2.1	<i>Feature Correspondency</i>	<i>6</i>
2.2.2	<i>Threshold setting.....</i>	<i>7</i>
2.2.3	<i>Running Time.....</i>	<i>8</i>
2.2.4	<i>Error measurement</i>	<i>8</i>
2.3	Implementation.....	8
3	Result.....	8
3.1	Smoke videos	9
3.1.1	<i>Smoke from burning kerosene (video 1).....</i>	<i>9</i>
3.1.2	<i>Smoke from burning plastic (video 2).....</i>	<i>10</i>
3.1.3	<i>Smoke from burning wood (video 3).....</i>	<i>12</i>
3.2	People video (video 4).....	13
3.3	Methane gas videos	15
3.3.1	<i>Methane gas video (video 5).....</i>	<i>15</i>
3.3.2	<i>Methane gas and people video (video 6).....</i>	<i>18</i>
4	Discussion.....	21
5	Conclusion.....	22
	Acknowledgements	22
	References.....	22

1 Introduction

In recent years, video surveillance has got the extensive application in many fields such as law enforcement, security, immigration, correctional institutions, and protection of the environment [10], etc. Using video surveillance to monitor and detect the smoke and gas is becoming more and more popular. Conventional smoke detectors normally detect the presence of combustion products by ionization or photometry based sensors [7]. But such detectors have some shortcomings. For one thing, sensors are limited to the placement because they just can be placed on the ceiling. For another, it is time consuming in outdoor or open spaces because it takes a long time from the combustion products start burning to the smoke reaches the sensors [7]. Therefore, instead of using conventional smoke sensor, we can use video surveillance because it can be placed anywhere indoor or outdoor and do early detection of the smoke from forest fires.

In addition, video equipment technologies can be used to detect invisible gas as well as visible smoke. For example, Infrared (IR) high sensitivity equipment can operate invisible light spectrum, thus IR cameras are used to detect the leakage of gas and volatile organic compounds (VOCs) including a range of hazardous and greenhouse gases [6].

Smoke and gas are the flowing characteristic of the suspended aerosol, so they have many dynamic features and the motion of smoke or gas plays an important role in video smoke or gas detection, furthermore, motion provides a clue of image understanding much than intensity, color, texture and others [16]. In order to detect this motion object, we usually use the approaches of Background Subtraction, Temporal Difference and Optical Flow. Background subtraction can extract the dynamic object information easily when the scene of video is static, temporal difference has strong self-adaptive ability for motion environment, but it cannot obtain all related characteristic pixels [13].

Optical flow method is widely used as it can get the relation or information of most pixels in both static and moving video, and the motion objects like smoke and gas can be detected without any scene information. Nevertheless, optical flow method is usually used with other approaches in real time video surveillance system on account of a majority of real time video surveillance basically monitors statically and optical flow method need complex calculations.

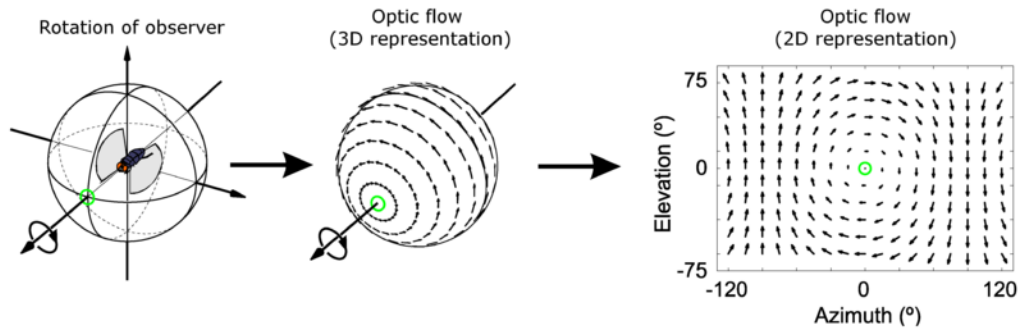


Figure 1. Optical flow [14]

Figure 1 illustrates the concept that 2D representation of optical flow is a perspective projection of the 3D velocities of surface points onto the image plane, and we will calculate the optical flow from spatiotemporal patterns of image intensity [9]. There are many optical flow techniques, and S. S. Beauchemin and J. L. Barron [15] divided them into six classes, intensity-based differential methods, multi-constraint methods,

frequency-based methods, correlation-based methods, multiple motion methods and temporal refinement methods. Among of them, the intensity-based differential methods are used mostly and the typical differential methods are Horn–Schunck method [5] and Lucas–Kanade method [4]. In this paper, I will analyze those two methods and one of the correlation-based methods called Anandan method for determining optical flow.

1.1 Aim

The aim of this research is to make a comparison of three main methods of estimating optical flow, included Horn–Schunck method, Lucas–Kanade method and Anandan method, with different criteria and test which algorithm is suited to detect smoke or gas in specific videos in a best way.

1.2 Background

In the background part, the relevant academic background for three estimating optical flow method – Horn Schunck method, Lucas Kanade method and Anandan method, and one of the comparison methods will be described in detail.

1.2.1 Optical flow constraint equation

As Andrés Bruhn, et al [1] said many differential methods of optic flow estimation base on brightness constancy and they suppose that the grey values of image objects (surface radiance) in subsequent frames is constant. As shown in Figure 2, gray value of the tracked pixel is unchanged over time.

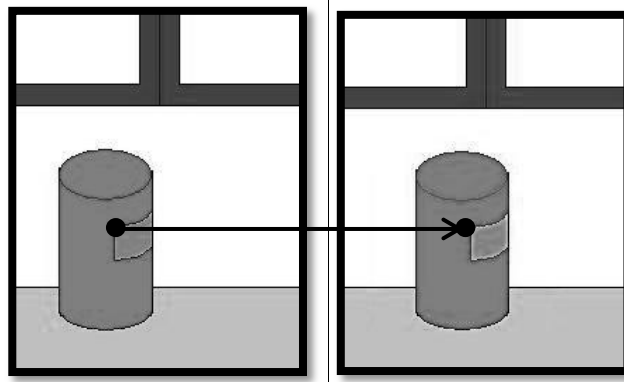


Figure 2. Brightness constancy

The image constraint equation can be given:

$$I(x, y, t) = I(x + dx, y + dy, t + dt) \quad \text{Eq. (1)}$$

Where it is for a 2D + t dimensional case, a voxel at location (x, y, t) with gray value $I(x, y, t)$ moves dx , dy and dt between two frames of image, and after movement, the gray value of that voxel is $I(x + dx, y + dy, t + dt)$. If $dt \rightarrow 0$, the gray values of those two voxels regard as constant.

Then we assume the displacement of the image between two nearby instants is small and perform a first order Taylor expansion to Equation (1):

$$I(x + dx, y + dy, t + dt) = I(x, y, t) + \frac{\partial I}{\partial x} dx + \frac{\partial I}{\partial y} dy + \frac{\partial I}{\partial t} dt + \varepsilon \quad \text{Eq. (2)}$$

Due to $\varepsilon = 0$ in small movement, we will get:

$$\frac{\partial I}{\partial x} dx + \frac{\partial I}{\partial y} dy + \frac{\partial I}{\partial t} dt = 0 \quad \text{Eq. (3)}$$

Let $u = \frac{dx}{dt}$ and $v = \frac{dy}{dt}$ represent the optical flow of $I(x, y, t)$ in x and y direction, and $I_x = \frac{\partial I}{\partial x}$, $I_y = \frac{\partial I}{\partial y}$ and $I_t = \frac{\partial I}{\partial t}$ represent the derivatives of the image at (x, y, t) in the corresponding directions. Then the optical flow constraint equation is created

$$I_x u + I_y v + I_t = 0 \quad \text{Eq. (4)}$$

1.2.2 Aperture problem

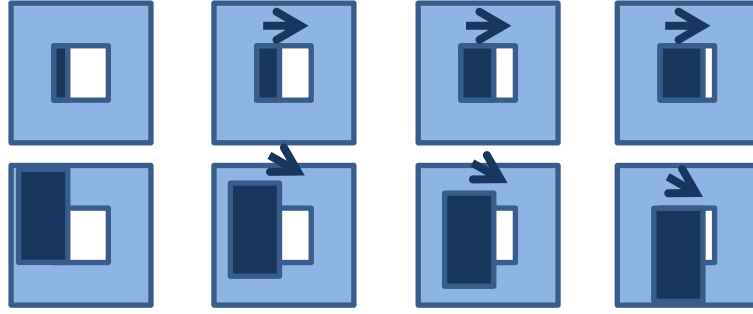


Figure 3. Aperture problem

The aperture problem normally arises from a moving object viewed through a small window, and it is impossible to determine the true orientation unless the end of the contour of object becomes visible in the aperture [8]. For example, the object seems to move from left to right in the first row of Figure 3. However, we can see in the second row, the true velocity is toward lower right and the component velocity in vertical direction is ignored. Obviously, the aperture problem has appeared in the Equation (4), two unknown constants u and v cannot be computed in single equation, so we need one more constraint equation.

1.2.3 Horn–Schunck method

Optical flow constraint equation cannot determine the unique optical flow of the images. Therefore, Horn and Schunck [5] put forward a smoothness constraint, which is a particular regularization term expressing the dependence and the expected smoothness of the flow field within the whole image.

From the smoothness constraint Equation (5) and optical flow constraint Equation (6):

$$E_s = \iint (u_x^2 + u_y^2 + v_x^2 + v_y^2) dx dy \quad \text{Eq. (5)}$$

$$E_c = \iint (I_x u + I_y v + I_t)^2 dx dy \quad \text{Eq. (6)}$$

We can know that optical flow should satisfy the global energy function (7):

$$E = \iint [(I_x u + I_y v + I_t)^2 + \alpha^2 (|\nabla u|^2 + |\nabla v|^2)] dx dy \quad \text{Eq. (7)}$$

Where the smoothness weight $\alpha > 0$ is the regularization parameter and the larger the values α , the stronger penalization of large flow gradients, thus the smoother the flow fields. In this paper, α equals to 1.

Equation (7) can be minimized by solving the associated Euler–Lagrange equations, and then we will obtain the component velocity (8) and (9) at last by iterating the minimized equation. In this paper, I use 100 iterations:

$$u^{k+1} = \bar{u}^k - \frac{I_x(I_x \bar{u}^k + I_y \bar{v}^k + I_t)}{\alpha^2 + I_x^2 + I_y^2} \quad \text{Eq. (8)}$$

$$v^{k+1} = \bar{v}^k - \frac{I_y(I_x \bar{u}^k + I_y \bar{v}^k + I_t)}{\alpha^2 + I_x^2 + I_y^2} \quad \text{Eq. (9)}$$

Where the superscript $k + 1$ point to the next iteration, and k is the result from last calculated.

1.2.4 Lucas–Kanade method

Different from global constraint in Horn–Schunck method, Lucas and Kanade [4] solve the aperture problem based on a local constraint. It assumes that the flow is essentially constant within a local area, and then it will implement a weighted least square fit by minimizing cost function (10):

$$\epsilon = \sum (\epsilon - \hat{\epsilon})^2 = \sum (I_x u + I_y v + I_t)^2, \epsilon = 0 \quad \text{Eq. (10)}$$

In order to minimize the cost function, get the derivative of Equation (10) and make it equal to 0:

$$\frac{\partial \epsilon}{\partial u} = \sum (I_x^2 u + I_x I_y v + I_x I_t) = 0 \quad \text{Eq. (11)}$$

$$\frac{\partial \epsilon}{\partial v} = \sum (I_y^2 u + I_x I_y v + I_y I_t) = 0 \quad \text{Eq. (12)}$$

Equation (11) and (12) can be formulated as a matrix (13)

$$\begin{pmatrix} \sum I_x^2 & \sum I_x I_y \\ \sum I_x I_y & \sum I_y^2 \end{pmatrix} \begin{pmatrix} u \\ v \end{pmatrix} = \begin{pmatrix} \sum I_x I_t \\ \sum I_y I_t \end{pmatrix} = 0 \quad \text{Eq. (13)}$$

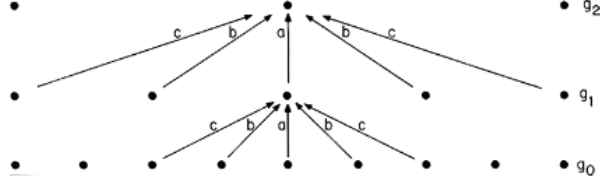
Let $M = \begin{pmatrix} \sum I_x^2 & \sum I_x I_y \\ \sum I_x I_y & \sum I_y^2 \end{pmatrix}$, $\vec{b} = \begin{pmatrix} \sum I_x I_t \\ \sum I_y I_t \end{pmatrix}$, if M is invertible, the optical flow (velocity) can be obtained as:

$$\vec{v} = M^{-1} \vec{b} \quad \text{Eq. (14)}$$

Otherwise, optical flow is calculated in flat regions where the image gradient vanishes.

1.2.5 Pyramid Lucas–Kanade method

Gaussian Pyramid is a low-pass pyramid, and it is generated by smoothing the images with a Gaussian filter firstly, and then subsampling the smoothed image by a factor of two along each coordinates direction, all the smoothed image are subjected to the same processing and it results in a yet smaller image [12], as Figure 3 shown.



$g_0 = \text{IMAGE}$

$g_L = \text{REDUCE}[g_{L-1}]$

Figure 3. Gaussian Pyramid [12]

Where g_0 is the original image, g_1 is the image after low-pass filter and subsampling g_0 . We can get the g_L image by processing g_{L-1} image and this process for each level is called “reduce”.

In fact Lucas-Kanade method is not efficient because we need large window which too often breaks the coherent motion assumption to catch large motions and it means the motions need to be small for the correct motion estimation. Therefore, we can use Gaussian pyramids (coarse to fine estimation method) to avoid this problem. We progress flow estimation from coarse to fine levels within Gaussian pyramids of the two images (current frame and subsequent frame), then warp or interpolate those fine flow back to the images level by level. In this paper, I will use the pyramid Lucas-Kanade method instead of Lucas-Kanada method and the pyramid level is three.

1.2.6 Anandan method

Anandan’s method [11] is based on a Laplacian pyramid and coarse-to-fine SSD (sum of squared difference)-based matching strategy. The Laplacian pyramid is very similar to Gaussian Pyramid, but it uses a Laplacian transform instead of a Gaussian filter, because it allows large displacement of object and enhances edges [11]. In this paper, it still implements the Gaussian Pyramid in Anandan’s method for making good comparison with pyramid Lucas-Kanade method and the pyramid level is two. The coarse-to-fine SSD measure is defined as

$$SSD_{1,2}(x; d) = \sum_{j=-n}^n \sum_{i=-n}^n W(i, j) [I_1(x + (i, j)) - I_2(x + d + (i, j))]^2 = W(x) * [I_1(x) - I_2(x + d)]^2 \quad \text{Eq. (15)}$$

Where $W(i, j)$ represents a discrete two-dimensional window function, $d = (d_x, d_y)$ is the velocity, the velocity is limited in the neighboring square region which size is $(2n + 1)$ and centered at two-dimensional value x .

1.2.7 Angular error

In most articles with regard to optical flow estimation [1] and [9], angular deviations are used to measure the errors. As written in [9], we present the velocity as 3-D direction vectors instead of 2-D, thereby the velocities are written as:

$$\vec{v} \equiv \frac{1}{\sqrt{(u^2 + v^2 + 1)}}(u, v, 1)^T \quad \text{Eq. (16)}$$

The angular error between the correct velocity v_c and an estimate velocity v_e is:

$$\psi E = \arccos(\vec{v}_c \cdot \vec{v}_e) \quad \text{Eq. (17)}$$

Barron et al. [8] also point out this error measure is convenient because it can handle both high and very low speeds without the amplification inherent in a correlative measure of vector differences, but it still has some bias.

2 Comparative method

In this chapter, I describe the selection of videos which contain smoke and gas. In addition, it is going to show a series of criteria or standards for comparisons among three different estimating optical flow methods, because the comparisons are based on primarily empirical test, and then concentrate on the accuracy reliability.

2.1 Selection of videos

Six videos will be selected as input material for comparison. Three videos contain smoke, two contain methane gas and one contains only people. The people video and three smoke videos are in color and the scenes are static. The smoke in smoke videos is from burning different combustion products and which means that the conditions of combustion are different. Two methane gas video are in gray scale because they are infrared videos. The scenes are moving and one video has not only methane gas but also moving people. In every video, I will choose ten frames to do the comparison in order to obtain more accurate values.

2.2 Criteria

There are four criteria for comparison among three different optical flow estimation methods and they are: feature correspondency, threshold setting, running time and error measurement. The reasons for choosing those criteria are as follows, firstly, the comparisons are based on observation and the direction of optical flow can be seen easily. Thus we can compare different methods by observing if the optical flows which are estimated by different methods are corresponding with the features. Secondly, as there are many moving objects in the videos, some optical flows are not from the smoke or gas. In order to select the right optical flows, it is necessary to set the threshold. Furthermore, the running speed is also important when comparing algorithms. We will calculate the running time of each method in different videos. Last but not least, following the scientific researchers who estimate or perform the optical flow methods [1], [9], I will also calculate the angular error between the estimated optical flow and correct optical flow. Better method with less error, therefore, the error measurement will be the last criteria in my comparison.

2.2.1 Feature Correspondency

Generally speaking, smoke and gas move upward and slowly, the shape of them will change with the passing of time. We will use these characteristic to separate the smoke from other motion object. For example, people will move back and forth and usually move faster than smoke. Moreover, the shape of people will not change. Thus, the features of smoke and gas will serve as the standard, and by comparing each method with this criterion, we can find out which method is more suitable to estimate optical flow of irregularly shaped object, which method is in reverse good at estimating optical flow for unchanged shape object. We can also find out the method is more appropriate for detecting object moves upward and in a slow pace. However, the judgment which is based on this criterion may not correct when the scenes is moving. Because when the scene is static, the static objects in videos should have not optical flow, the apparent optical flow must from the moving object such as smoke or gas.

But if the scene is moving downward, all the things inside the scene are moving upward and optical flows are not totally from smoke or gas. In this case, we cannot make a correct judgment for which method is better. Therefore, a new criterion appears to solve the problem that estimating optical flow in dynamic scene videos, it is threshold.

2.2.2 Threshold setting

In dynamic scene videos, the threshold value will be set for removing the interference from moving scene. Interference denotes the optical flows which are produced by the moving scene and it will hinder the comparison. I have set two thresholds, one is used to determine which flow is interference, and the other is used to reduce the interference.

$$\max_flow/current_flow < Theshold_1 \quad \text{Eq. (18)}$$

$$R = Theshold_2 * \max_flow \quad \text{Eq. (19)}$$

Where R is the reduce value. Usually Theshold₁ is between 2 to 3, it means if the current flow is larger than half or one third of max flow, it should be the interference. Theshold₂ is from 0.5 to 0.9, we reduce the interference by subtract a part of max value.

The details of how to reduce interference are as follow. First of all, calculate the average value among all optical flows. Because most optical flows presented in moving scene are interferences and average value tends to most value, so the direction of average value are the same as the directions of interferences. And if the direction of one optical flow is not the same as the direction of average value, we can eliminate this optical flow as interference. Otherwise, it can be the interference and goes to the next step.

We find out the maximum value among the optical flows which has the same direction as average value. Here is an example to calculate the maximum value of component velocity u :

```
if ((av_u/Ax(i,j)) > 0 && abs(Ax(i,j)) > abs(max_u))
    max_u = Ax(i,j);
```

Where av_u is the average value of component velocity u , $Ax(i, j)$ is current component velocity u in i row and j column, max_u is the maximum value of component velocity u and abs is method to get the absolute value.

Use maximum velocity in Equation (18), if the currently velocity is satisfied with Equation (18), it should be regarded as interference. The maximum value will be used in classification, because I find that most values of interferences are close to the value of maximum velocity which has the same direction as average velocity.

Lastly, we can reduce the interference in two cases. One is the easier case that the interference is just in one direction (horizontal or vertical direction) and one of the component velocities is equal to zero. The other is more difficult that the interference is slanting and the values of both component velocities are not equal to zero. And then use Equation (19) in two different cases. In case one, we just use Equation (19) to reduce the interference in one component velocity. In case two, we need to reduce the interference in both two component velocities. Here is the example to reduce the interference in horizontal direction and it just need to calculate the correct component velocity u , velocity v is equal to zero:

```

if ((Ax(i,j)-sub_u)/Ax(i,j)<0)
    Ax(i,j)=0;
else
    Ax(i,j)=Ax(i,j)-sub_u;

```

Where sub_u is R in Equation (19). If after reduce sub_u , current component velocity $Ax(i,j)$ will change its direction, $Ax(i,j)$ will be set to zero. Otherwise, $Ax(i,j)$ is equal to the difference between current component velocity and reduce number.

2.2.3 Running Time

In real time video surveillance, quick detection of results pays an important role. Calculate the running time in an easy way for each frame, get the CPU (central processing unit) time before and after running the optical flow method, then subtract the former time from the latter time and we will get the running time, the average running time is the sum of each frame divided by the number of frames, the pseudo code is following.

```

Running_time = 0;
for k = 1 : nFrames
    gettime = cputime;
    ..... (run the function)
    Running_time = Running_time + cputime - gettime;
end
Runnning_time = Running_time / (nFrames);

```

Where $nFrames$ is the number of frames.

2.2.4 Error measurement

Angular measure of error will be used as a criterion in this paper, the average angular error and standard deviation between the correct velocity and an estimate velocity will be calculated. A smaller standard deviation represents those angular errors that close to the average angular error. It is a good way to compare three different optical flow estimation methods for better estimation method will provide less angular error. However, it is very difficult to find the correct velocity. Therefore, the estimate velocity from each method will be considered as correct velocity once, and calculate the average angular error with the estimate velocity from another method and itself. The reason why to calculate the average angular error between the method and itself is that the result of it is not equals to zero and it can be a reference. But during the comparison, this result should be ignored because it holds lowest angular error.

2.3 Implementation

All the optical flow methods and the comparative methods will be implemented by using MATLAB®.

3 Result

In this section, I will classify the result into three different types - the smoke type, people type and methane gas type. In smoke type, there are three different videos with different kind of smokes, in methane gas type, there are two different videos, and in

people type, just one video, but one of the methane gas videos also contains people. In addition, only the methane gas videos use threshold values for dealing with the moving scene.

In each result part of videos, it has at least one table and three images. The tables will show the average running time of each method for different methods. At the same time, the average error and standard deviation between the reference method and the other method will be presented in the tables. Optical flows which are estimated by three methods will be displayed by images.

3.1 Smoke videos

3.1.1 Smoke from burning kerosene (video 1)

Table 1. Comparison based on video 1, frame from 53 to 62

Reference Method	Average Running Time/s	Method	Average Error/degree	Standard Deviation/degree
Horn–Schunck method (iteration = 100)	1.398438	Horn–Schunck method	37.9095	29.7522
		Lucas–Kanade method	54.2633	24.7589
		Anandan method	57.6292	26.5610
Lucas–Kanade method (pyramid level = 3)	22.257813	Horn–Schunck method	62.6600	29.6502
		Lucas–Kanade method	50.6761	37.3537
		Anandan method	64.4549	32.9627
Anandan method (pyramid level = 2)	118.189063	Horn–Schunck method	60.3821	33.1226
		Lucas–Kanade method	58.8111	35.4061
		Anandan method	45.0323	37.5245

It is clear from Table 1 that Horn–Schunck method is the fastest method and Anandan method is the slowest one even though it just implements two level of pyramid compared with Lucas–Kanade method which has implemented three level of pyramid. Besides, Lucas–Kanade method holds least error and standard deviation and Anandan method holds most in this case.

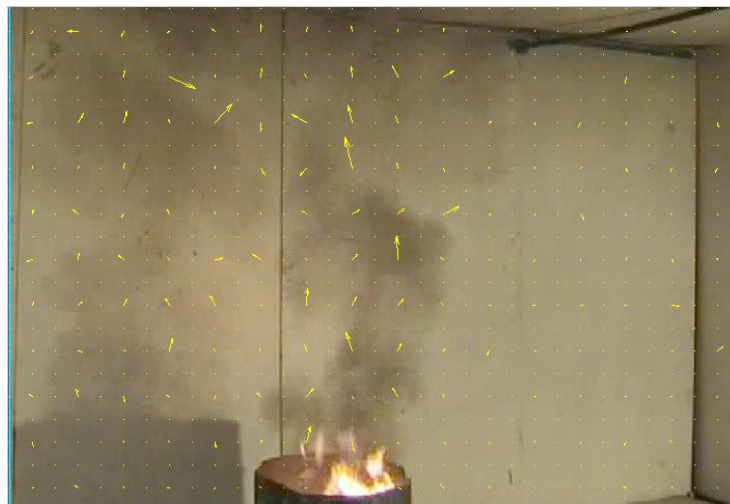


Figure 4(1). Frame 62 with Horn–Schunck method in video 1

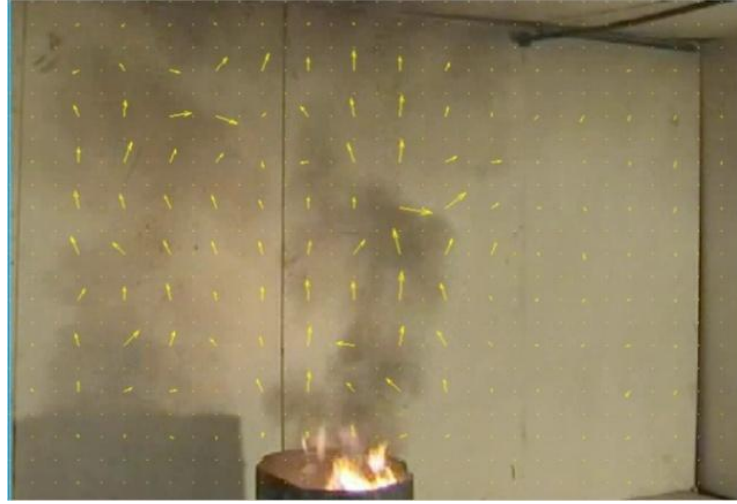


Figure 4(2). Frame 62 with Lucas-Kanade method in video 1

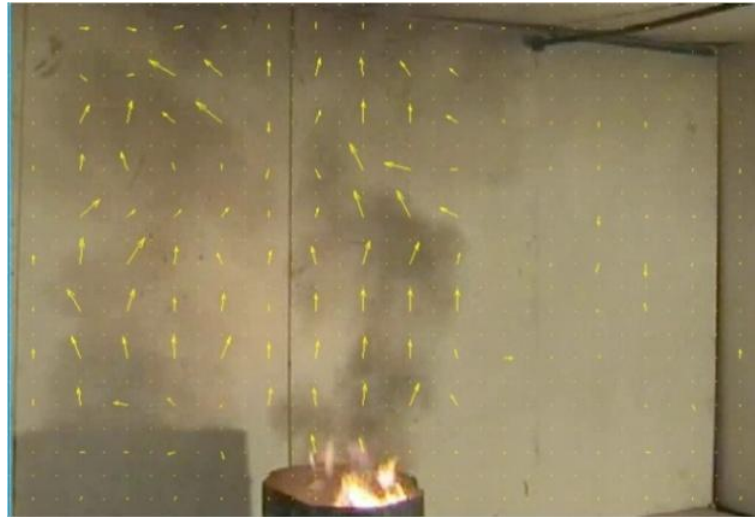


Figure 4(3). Frame 62 with Anandan method in video 1

From Figure 4(1-3), we can see that the result of both the Lucas-Kanade method and the Anandan method are better than the result of the Horn-Schunck method in this video.

3.1.2 Smoke from burning plastic (video 2)

Table 2. Comparison based on video 2, frame from 53 to 62

Reference Method	Average Running Time/s	Method	Average Error/degree	Standard Deviation/degree
Horn-Schunck method (iteration = 100)	1.857813	Horn-Schunck method	23.5764	24.2645
		Lucas-Kanade method	34.6794	25.1356
		Anandan method	32.0709	24.5307
Lucas-Kanade method (pyramid level = 3)	27.331250	Horn-Schunck method	49.8003	28.8337
		Lucas-Kanade method	38.6974	33.5852
		Anandan method	50.2495	29.8629
Anandan method (pyramid level = 2)	140.606250	Horn-Schunck method	21.9047	28.8409
		Lucas-Kanade method	28.8409	31.8254
		Anandan method	13.4102	25.4198

Different from Table 1, Lucas–Kanade method has most error and standard deviation in Table 2. And Horn–Schunck method has least error and standard deviation.

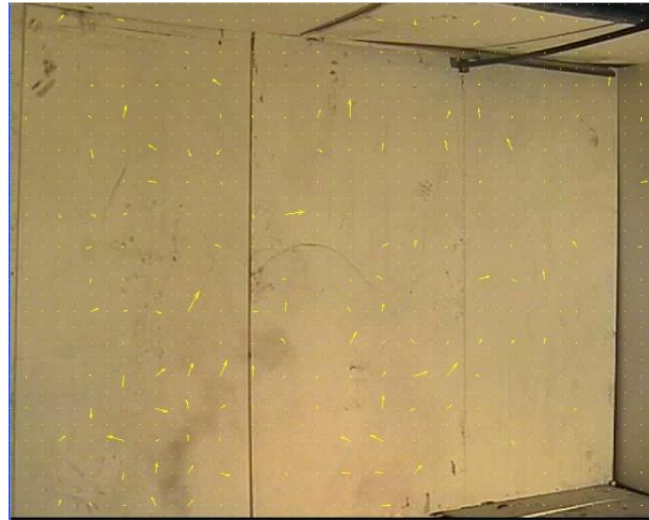


Figure 5(1). Frame 62 with Horn–Schunck method in video 2



Figure 5(2). Frame 62 with Lucas–Kanade method in video 2



Figure 5(3). Frame 62 with Anandan method in video 2

Anandan method (Figure 5(3)) gives a better result than any other method in video 2.

3.1.3 Smoke from burning wood (video 3)

Table 3. Comparison based on video 3, frame from 680 to 689

Reference Method	Average Running Time/s	Method	Average Error/degree	Standard Deviation/degree
Horn–Schunck method (iteration = 100)	1.873438	Horn–Schunck method	6.7525	14.3249
		Lucas–Kanade method	13.0921	19.5246
		Anandan method	9.3352	16.3094
Lucas–Kanade method (pyramid level = 3)	27.496875	Horn–Schunck method	26.8236	25.4911
		Lucas–Kanade method	20.4840	25.4774
		Anandan method	27.2269	25.7516
Anandan method (pyramid level = 2)	144.903125	Horn–Schunck method	4.7083	14.0971
		Lucas–Kanade method	8.8684	19.4247
		Anandan method	2.1255	10.6510

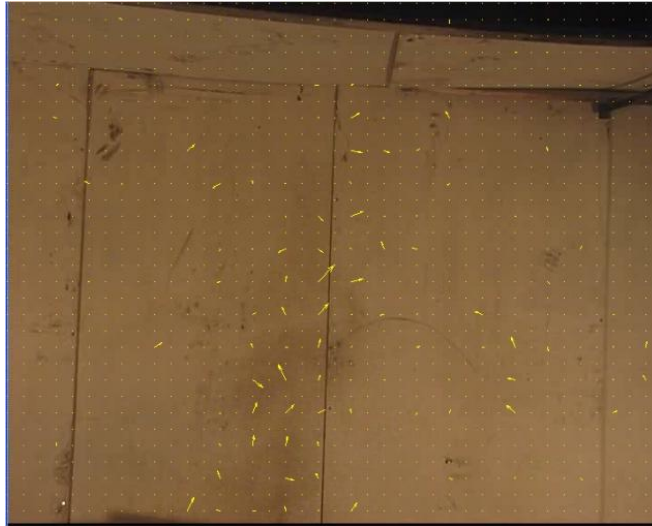


Figure 6(1). Frame 680 with Horn–Schunck method in video 3

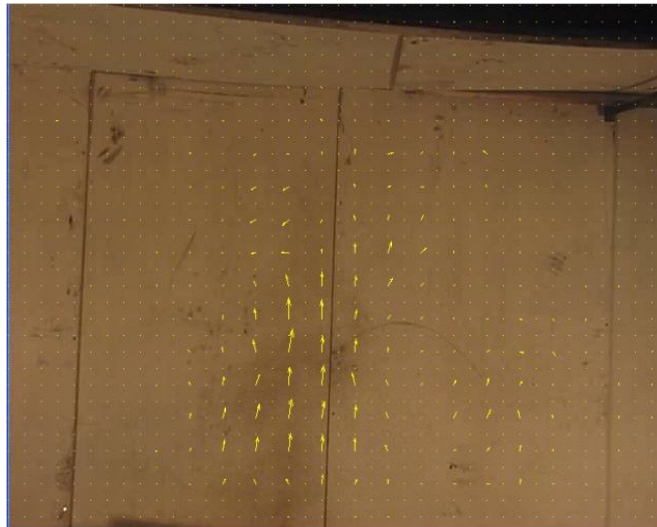


Figure 6(2). Frame 680 with Lucas–Kanade method in video 3

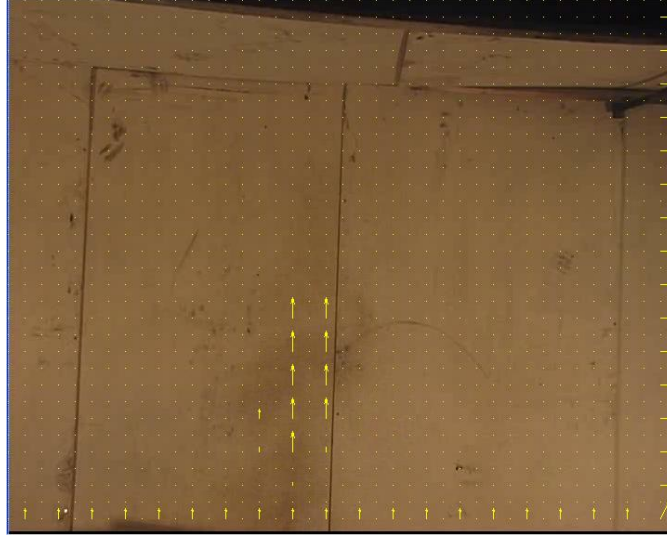


Figure 6(3). Frame 680 with Anandan method in video 3

All the results of video 3 including Table and Figures are similar to the results of video2. I can draw a short conclusion by analyzing the results of three videos above. Above all, Horn–Schunck method runs fastest and usually has least error and standard deviation, but the flows from it are not represented in a good way. On the contrary, although Anandan method needs more time to run, the results of it are presented very well. Meanwhile, Lucas–Kanade method is situated between of them with the mean values of both running time and results.

3.2 People video (video 4)

Table 4. Comparison based on video 4, frame from 280 to 289

Reference Method	Average Running Time/s	Method	Average Error/degree	Standard Deviation/degree
Horn–Schunck method (iteration = 100)	1.455966	Horn–Schunck method	40.0045	29.3470
		Lucas–Kanade method	51.5040	24.4146
		Anandan method	58.5323	29.6075
Lucas–Kanade method (pyramid level = 3)	22.490057	Horn–Schunck method	60.7707	30.0135
		Lucas–Kanade method	49.2712	37.1465
		Anandan method	69.4275	36.3572
Anandan method (pyramid level = 2)	125.258523	Horn–Schunck method	58.3453	37.3441
		Lucas–Kanade method	61.0444	41.2836
		Anandan method	40.6848	37.3276

The values for average error and standard deviation from Anandan method are larger than the other two methods as indicated in Table 4.



Figure 7(1). Frame 280 with Horn-Schunck method in video 4



Figure 7(2). Frame 280 with Lucas-Kanade method in video 4



Figure 7(3). Frame 280 with Anandan method in video 4

Figure 7 (1 to 3) show that Horn-Schunck method and Lucas-Kanade method can estimate the flows in horizontal direction in a good way, while Anandan method presents some wrong flows in that direction, and we can compare the flows within the red circle in figures.

3.3 Methane gas videos

Because methane gas cannot be seen with the naked eye, we use infrared videos to observe methane gas and they are dealt with in form of gray scale images. Different from the videos above, the scenes of infrared videos below are moving.

3.3.1 Methane gas video (video 5)

Table 5. Comparison based on video 5, frame from 805 to 814

Reference Method	Average Running Time/s	Method	Average Error/degree	Standard Deviation/degree
Horn–Schunck method (iteration = 100)	0.837500	Horn–Schunck method	13.7408	17.7958
		Lucas–Kanade method	21.3343	20.8581
		Anandan method	21.0542	23.6675
Lucas–Kanade method (pyramid level = 3)	13.445313	Horn–Schunck method	37.7151	29.2655
		Lucas–Kanade method	30.1217	31.4389
		Anandan method	42.9899	34.9819
Anandan method (pyramid level = 2)	54.757813	Horn–Schunck method	16.7331	25.4262
		Lucas–Kanade method	22.2880	33.4000
		Anandan method	9.4197	18.5040

Horn–Schunck method has less error and at the same time, Lucas–Kanade method has most error as showed in Table 5.

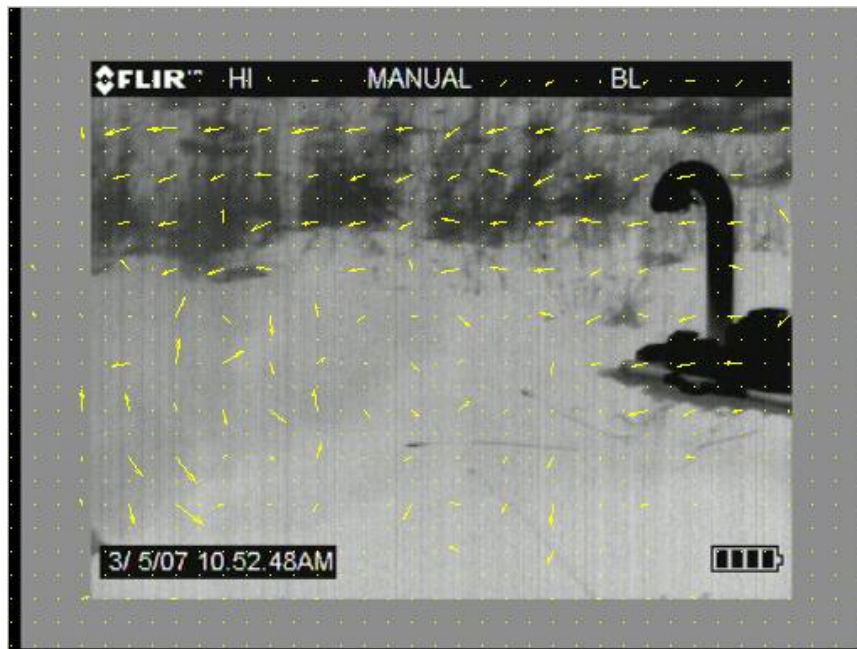


Figure 8(1). Frame 805 with Horn–Schunck method in video 5

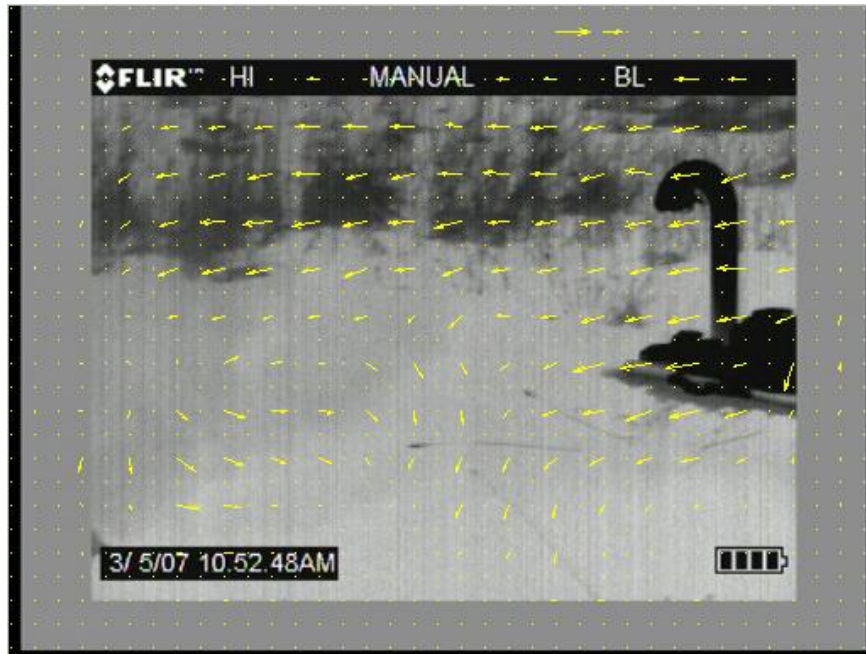


Figure 8(2). Frame 805 with Lucas–Kanade method in video 5

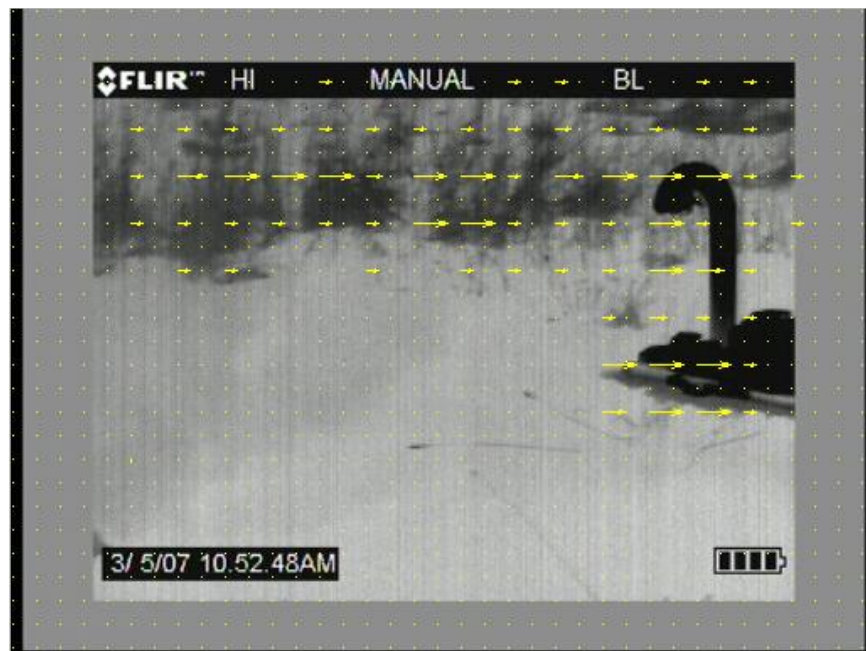


Figure 8(3). Frame 805 with Anandan method in video 5

The scene of this video is moving toward right, so it leads to the flows of most objects point to left. However, we can focus on the Figure 8 (3) and the flows which are estimated by Anandan method are in wrong direction. This kind of mistake occurred in video 4 above.

Apparently, what we need to do is to reduce the disturbance from moving scene and achieve the right optical flows. Therefore, we need to remove the obstacles by setting the threshold value. The results below are the right flows after process with threshold.



Figure 9(1). Frame 805 with Horn-Schunck method in video 5 after reduce interference
First threshold value is 2, second value is 0.9



Figure 9(2). Frame 805 with Lucas-Kanade method in video 5 after reduce interference
First threshold value is 2, second threshold value is 0.9



Figure 9(3). Frame 805 with Anandan method in video 5 after reduce interference
First threshold value is 4, second threshold value is 0.9

Both Horn–Schunck method and Lucas–Kanade method estimate good optical flows except for Anandan method. The first threshold value of Anandan method is four while the first threshold values of Horn–Schunck method and Lucas–Kanade method are just two, it means the influence of interference is large in Anandan method.

3.3.2 Methane gas and people video (video 6)

Table 6. Comparison based on video 6, frame from 53 to 62

Reference Method	Average Running Time/s	Method	Average Error/degree	Standard Deviation/degree
Horn–Schunck method (iteration = 100)	1.312500	Horn–Schunck method	13.7839	14.3898
		Lucas–Kanade method	21.7770	16.9393
		Anandan method	17.4768	13.5776
Lucas–Kanade method (pyramid level = 3)	20.446875	Horn–Schunck method	43.5916	29.4502
		Lucas–Kanade method	35.5985	33.7140
		Anandan method	43.4365	30.1943
Anandan method (pyramid level = 2)	88.867188	Horn–Schunck method	16.7953	19.0250
		Lucas–Kanade method	20.9404	22.9143
		Anandan method	13.1024	19.1437

Table 6 indicates that Anandan method has least error and Horn–Schunck method has most error in this video

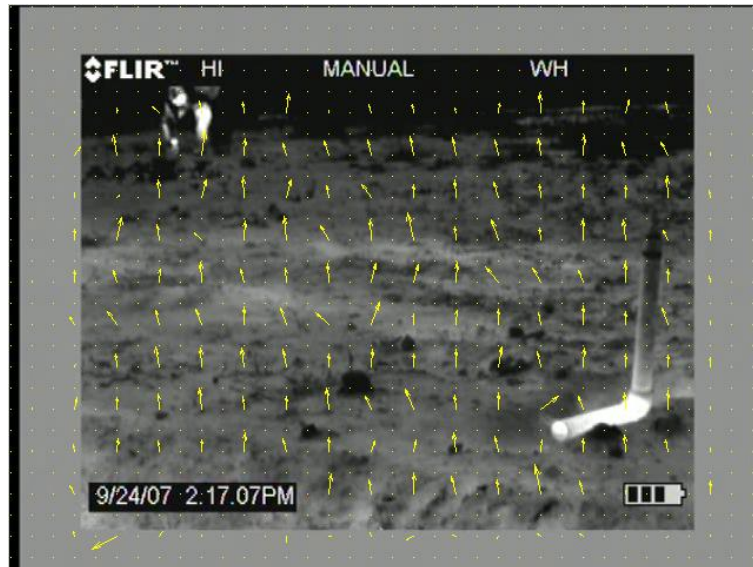


Figure 9(1). Frame 53 with Horn–Schunck method in video 6

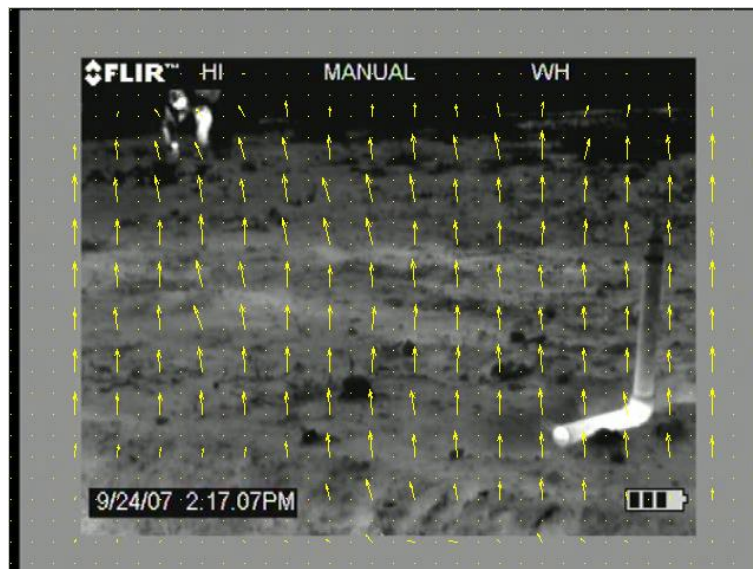


Figure 9(2). Frame 53 with Lucas–Kanade method in video 6

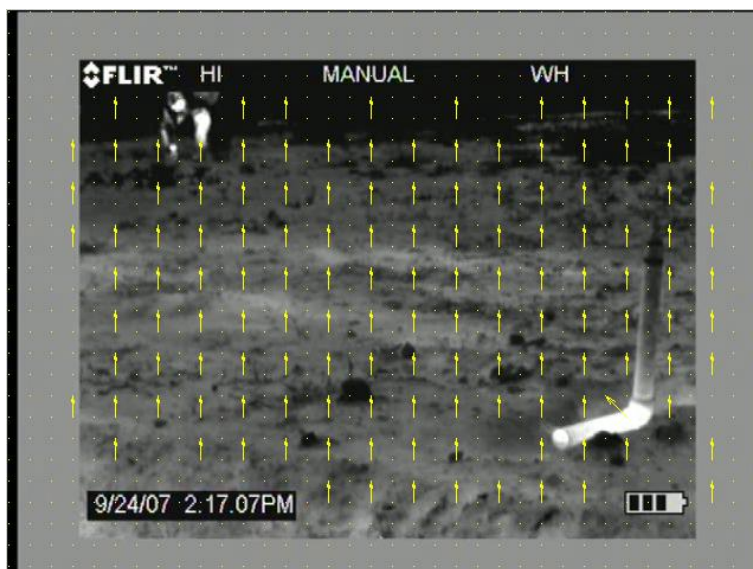


Figure 9(3). Frame 53 with Anandan method in video 6

As we can see, from frame 53 to frame 54 in video 6, the background is moving downward, and it leads to all the objects in screen are moving upward. We use threshold value to get the right optical flows. The results are as below:

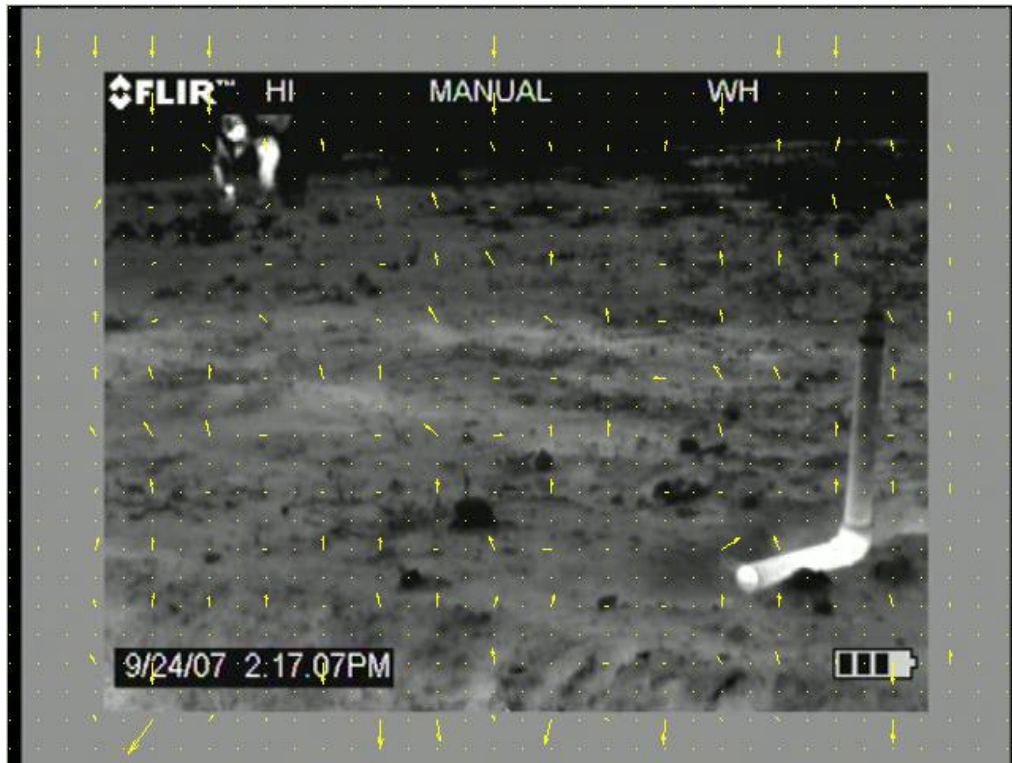


Figure 10(1). Frame 53 with Horn-Schunck method in video 6 after reduce interference
First threshold value is 3, second threshold value is 0.75

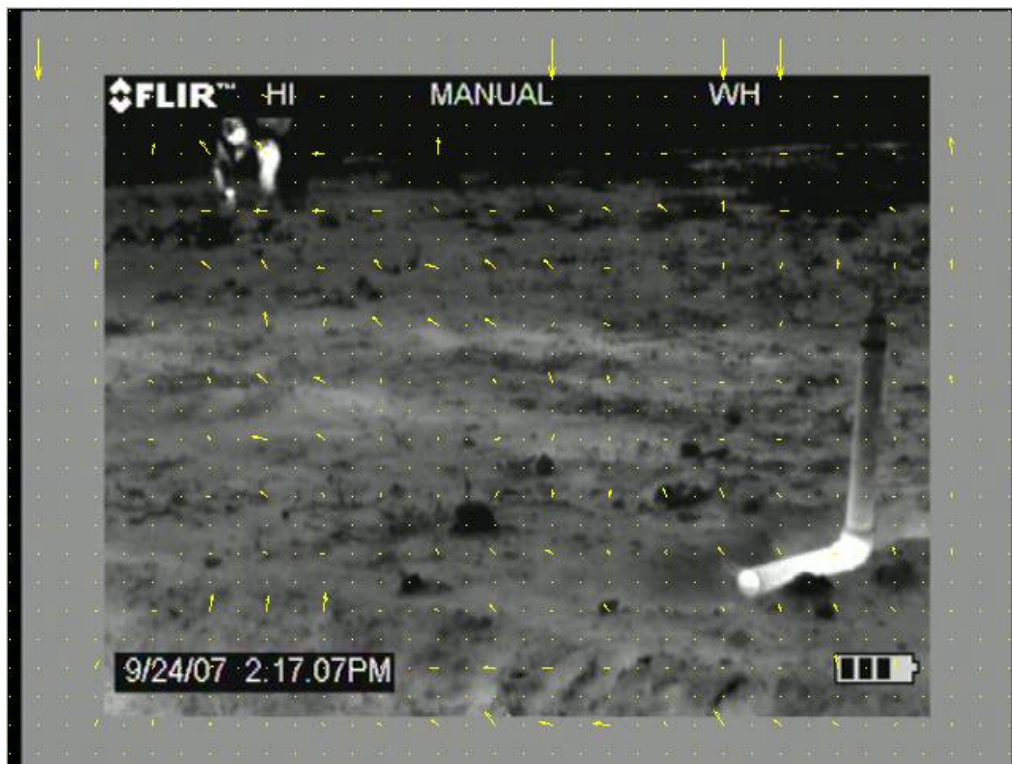


Figure 10(2). Frame 53 with Lucas-Kanade method in video 6 after reduce interference
First threshold value is 3, second threshold value is 0.75

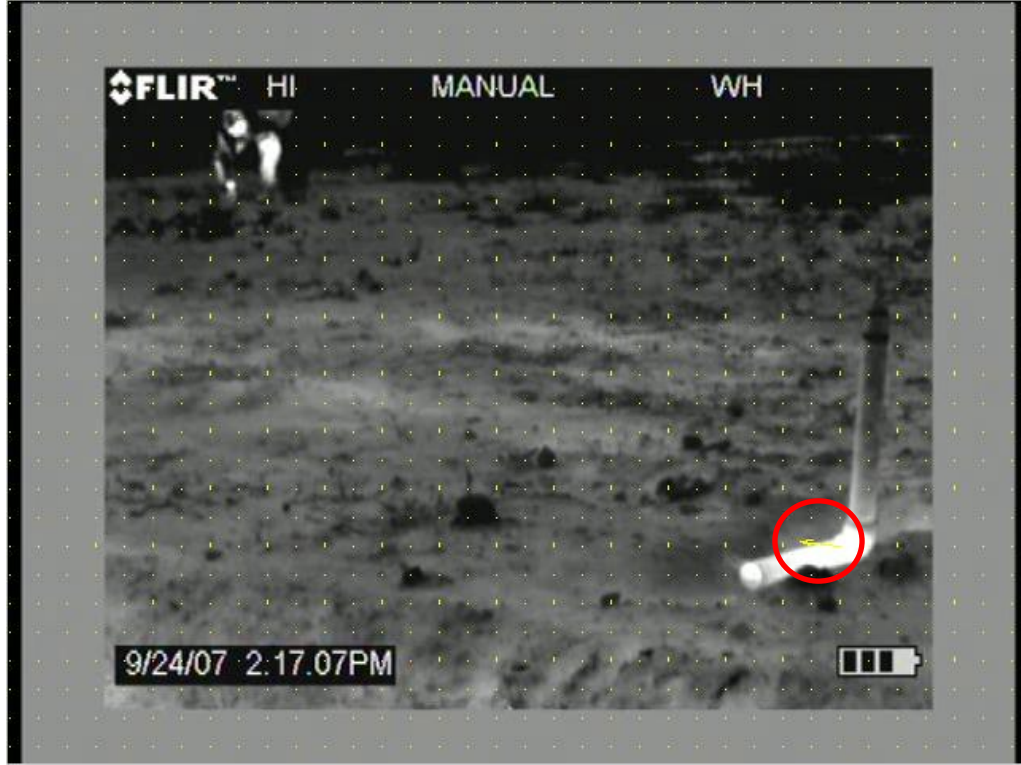


Figure 10(3). Frame 53 with Anandan method in video 6 after reduce interference
First threshold value is 3, second threshold value is 0.9

From Figure 10 (1 to 3), we realize that Horn–Schunck method gives most correct optical flows, but there is just one optical flow left after reduce interference in Anandan method.

4 Discussion

After compare different optical flow method, we can realize those kinds of methods can be used in video processing in a good way, and I would like to discuss the pros and cons of those three methods. From the result, I find that Horn–Schunck method, which is a fast method, is very suitable to estimate the optical flow of objects whose gray value is close to background's gray value. In other words, it is good to be used in infrared videos. The advantage of Anandan method is that estimating the optical flow from the upward moving objects very easily. However, it wastes time and it is not suited for infrared videos. Chen Bangzhong etc. [3] held the same opinion that in infrared image sequences, Horn-Schunck method has the best performance while Anandan has the worst among six different optical flow methods in their paper. The results of the Lucas–Kanade method are relatively steady and its advantage is that it can measure the flows in every direction. However, the effect figures of Lucas–Kanade method are not better than the figures of Anandan method in smoke video and in infrared videos, Horn–Schunck method can be used more suitably than Lucas–Kanade method.

The result seems to be satisfying, but the precision of it still need to be improved. For one thing, the running time of each method highly depends on the code of program or we can say the time complexity of each algorithm in each optical flow method, because different algorithms can be realized in different ways and it is difficult to find out the most timesaving way. For example, Chen Bangzhong etc. [3] presented the calculation quantities of Lucas–Kanade method are the least, while Anandan method are the largest and Horn–Schunck method is between those two

methods. But in my paper, Horn–Schunck method run fastest while Anandan method run the slowest and Lucas–Kanade method is between them. For the other thing, although calculate the angular error is a nice approach to compare different optical flow method, finding out the reference of correct velocity is demanding. Scientific researchers usually use this method when he or she has the correct velocity of the video, such as [1] and [9].

5 Conclusion

The conclusion I draw from my research is that it seems like the best choice is the Anandan method when measuring the flow in general digital video containing smoke. Because the results of Anandan method show that this method is very good at estimating the optical flow of smoke, although it runs a long time.

However, if the general digital video contains people as well as smoke, my suggestion is to use Lucas–Kanade method instead of Anandan method. Combined the smoke videos with the people video, it is obvious that the Anandan method can estimate the optical flow from the upward moving objects easily, while Horn–Schunck method is more suited to detect the objects which move back and forth and Lucas–Kanade method can estimate the optical flow in any direction.

Lastly, if the video is an infrared video then the results in my paper leans more at that the Horn–Schunck method should be a better method. Because Horn–Schunck method is best with fast running time, good results and with least angle error in methane gas videos (infrared videos). It is seems to very hard for Anandan method to estimate the optical flow in infrared videos. And Lucas–Kanade method is between them.

Acknowledgements

I would like to thank my supervisor Julia for her valued support and encouragement in the past few weeks. I also appreciate my examiner Stefan who provides precious views and suggestions for this paper.

References

- [1] A. Bruhn, J. Weickert, and C. Schnörr, “Lucas/Kanade meets Horn/Schunck: combining local and global optic flow methods”, *International Journal of Computer Vision (IJCV)*, 61(3), February 2005, pp. 211–231.
- [2] A. Safitri, X. Gao and M. S. Mannan, “Dispersion modeling approach for quantification of methane emission rates from natural gas fugitive leaks detected by infrared imaging technique”, *Journal of Loss Prevention in the Process Industries*, 24(2), March 2011, pp. 138-145.
- [3] B. Chen, X. Wang, J. Tu and Y. Peng, “Moving Target Detection from Infrared Image Sequences”, *Journal of Detection & Control*, 24(3), 2002, pp. 11-13,20
- [4] B. D. Lucas and T. Kanade, “An Iterative Image Registration Technique with an Application to Stereo Vision”, *Proceedings of the 1981 DARPA Image Understanding Workshop*, April 1981, pp. 121-130.
- [5] B. K. P. Horn and B. G. Schunck, “Determining Optical Flow”, *Artificial Intelligence*, 17(1-3), 1981, pp. 185-203.
- [6] FLIR Systems AB, “IR camera detects gas leaks and measures temperature”, *Sealing Technology*, 2009(8), August 2009, p. 12.

- [7] F. Yuan, "Video-based smoke detection with histogram sequence of LBP and LBPV pyramids", *Fire Safety Journal*, 46(3), April 2011, pp. 132-139.
- [8] I. Murakami, "The aperture problem in egocentric motion", *Trends in Neurosciences*, 27(4), 2004, pp. 174-177.
- [9] J. L. Barron, D. J. Fleet and S. S. Beauchemin, "Performance of optical flow techniques", *International Journal of Computer Vision*, 12(1), 1994, pp.43-77.
- [10] M. Nieto, K. Johnston-Dodds and C. W. Simmons, "Public and Private Applications of Video surveillance and Biometric Technologies, California Research Bureau", California State Library, California Research Bureau, 2002.
- [11] P. Anandan, "A computational framework and an algorithm for the measurement of visual motion", *International Journal of Computer Vision*, 2(3), 1989, pp.283-310.
- [12] P. Burt, and E. Adelson, "The Laplacian Pyramid as a Compact Image Code", *IEEE Transactions on Communications*, 31(4), Apr 1983, pp.532 – 540.
- [13] Q. Luo, N. Han, J. Kan and Z. Wang, "Effective Dynamic Object Detecting for Video-based Forest Fire Smog Recognition", *Image and Signal Processing*, 2009. CISP '09. 2nd International Congress on, 2009, pp.1-5.
- [14] S. J. Huston and H. G. Krapp, "Visuomotor Transformation in the Fly Gaze Stabilization System", *PLoS Biol*, 6(7), 2008, p.173
- [15] S. S. Beauchemin and J. L. Barron, "The computation of optical flow", *Journal ACM Computing Surveys (CSUR)*, 1995, pp.433-467
- [16] Z. Pan and J. J. Pfeiffer, Jr., "Adaptive estimation of optical flow from general object motion", *Proceeding SAC '92 Proceedings of the 1992 ACM/SIGAPP Symposium on Applied computing: technological challenges of the 1990's*, 1992.